



ELSEVIER

Contents lists available at SciVerse ScienceDirect

Biosensors and Bioelectronics

journal homepage: www.elsevier.com/locate/bios

Label-free detection of single-nucleotide polymorphisms associated with myeloid differentiation-2 using a nanostructured biosensor

Yu-Ting Chin^a, En-Chih Liao^b, Chia-Che Wu^a, Gou-Jen Wang^{a,c,d,*}, Jaw-Ji Tsai^{b,**}

^a Department of Mechanical Engineering, National Chung-Hsing University, Taichung 40227, Taiwan

^b Department of Medical Education and Research, Taichung Veterans General Hospital, Taichung 40705, Taiwan

^c Graduate Institute of Biomedical Engineering, National Chung-Hsing University, Taichung 40227, Taiwan

^d Ph.D. Program in Tissue Engineering and Regenerative Medicine, National Chung-Hsing University, Taichung 40227, Taiwan

ARTICLE INFO

Article history:

Received 22 April 2013

Received in revised form

11 May 2013

Accepted 28 May 2013

Available online 11 June 2013

Keywords:

Myeloid differentiation-2 (MD-2) gene

promoter

Single nucleotide polymorphism (SNP)

detection

Nanostructured biosensor

Electrochemical impedance spectroscopy

(EIS) analysis

ABSTRACT

House dust mites are the major source of indoor allergens that are responsible for asthma. The major dust mite allergen is the group II allergen, Der p2. Myeloid differentiation-2 (MD-2) acts as an essential component in the CD14-TLR4 (toll-like receptor)/MD-2 receptor complex for Der p2 recognition. Mutations of the MD-2 associated gene on chromosome 8 degrade a human's innate responses. In this study, we report the effective detection of mutations to the MD-2 gene promoter, using a sensitive nanostructured biosensor with a sensing electrode of gold nanoparticles (GNPs) uniformly deposited in a nanohemisphere array. The 70 mer MD-2 expressed gene fragment was used to probe gene mutation. The complementary target, containing 156 mer nucleotide, was prepared using the fresh blood from patients with allergic disease. A total of 37 target samples, including 19 gene mutated samples and 18 normal samples, were prepared by a 20 cycles PCR process, and used for discrimination experiments. Experimental results illustrated that the nanostructured biosensor clearly discriminates between mutated and non-mutated MD-2 allergy genes.

© 2013 Elsevier B.V. All rights reserved.

1. Introduction

Common allergy related diseases include perennial allergic rhinitis, allergic asthma, perennial allergic conjunctivitis, atopic dermatitis, and urticaria. Among these, allergic rhinitis and asthma are the most common. The pathogenic mechanism is the inflammatory response, induced by the attachment of allergens in air to the epithelia of the respiratory tract. When people with allergies are exposed to allergens, a series of immune reactions, such as the mass production of immunoglobulin E (IgE) antibodies, eosinophilia, mast cell activation, and histamine production, are induced by the body. Allergic constitution is due to the activation of myeloid differentiation-2 (MD-2) in toll-like receptors (TLR), which is the main mechanism of pathogenic microorganism identification in a human's innate immune system. MD-2 binds to dust mite allergens, inducing allergic reactions. It has been reported that mutations of the MD-2 associated gene on chromosome 8 degrade a human's innate responses (Miyake, 2004). Gene

variation in the allergic innate immune receptors is due to single nucleotide (A, T, C or G) replacement polymorphisms, commonly called single nucleotide polymorphisms (SNPs). If gene variations in the allergic innate immune receptors are accurately detected, the early diagnosis of allergic pathogens and preventive treatment can be effectively achieved.

When two human genomes are compared, there is only 0.01% difference (Cooper et al., 1985). Most of these differences are SNPs. Almost all usual SNPs have only two alleles. Although SNPs generally occur more frequently in non-coding segments than in coding segments, a small variation in DNA sequences can affect humans' response to pathogens, chemicals, drugs, vaccines, and other agents, with implications in inducing severe disease. Several analytical methods have been implemented for the detection of known SNPs, including DNA sequencing (Altshuler et al., 2000), mass spectrometry (Griffin and Smith, 2000), capillary electrophoresis (Drabovich and Krylov, 2006), electrochemical analysis, denaturing HPLC, gel electrophoresis, and hybridization analysis.

Kerman et al. (2004) detected SNPs by observing the change in the oxide wave of monobase-modified colloidal gold nanoparticles (GNPs). When the mismatched bases were complementary to the monobase, a significant change in the Au oxide wave was detected. A label-free method for the detection of point mutations in short DNA samples, based on non-metallized silicon field-effect transistors (FET) in a microarray, was reported by Ingebrandt et al. (2007).

* Corresponding author at: Graduate Institute of Biomedical Engineering, National Chung-Hsing University, Taichung 40227, Taiwan. Tel.: +886 4 22840725x320; fax: +886 4 22877170.

** Corresponding author. Tel.: +886 4 23592525x4000; fax: +886 4 23592705.

E-mail addresses: gjwang@dragon.nchu.edu.tw (G.-J. Wang), jawji@vghctc.gov.tw (J.-J. Tsai).

The use of the differential AC readout concept enabled a reliable readout and the possibility for quick screening of large sensor arrays. Zhang et al. (2009) proposed a label-free and sensitive SNP detection approach, based on the integration of ligation-rolling circle amplification (L-RCA) and methylene blue intercalation; a detection limit of 40 amol mutated strands was achieved. An electrochemical method for multiplex SNP detection, without probe immobilization, was developed by Luo and Hsing (2009). A neutrally charged peptide nucleic acid (PNA) probe, labeled with an electroactive indicator and a negatively charged ITO electrode, was used for the immobilization-free detection of target DNA. Palchetti et al. (2010) demonstrated the feasibility of detecting hybridization of DNA target oligonucleotides, on a mixed monolayer of peptide nucleic acid and mercaptohexanol, using electrochemical impedance spectroscopy (EIS). Ensafi et al. (2011) detected cancer and chronic lymphocytic leukemia using a DNA impedance biosensor based on a gold-nanoparticle-modified electrode. An electrochemical biosensor for sensitive detection of the BRAF V600E mutation in colorectal cancer cells, based on a dual amplification strategy of amplification-refractory mutation system (ARMS) PCR and multiple enzyme labels, was developed by Situ et al. (2012). The proposed method was demonstrated to be more sensitive than DNA sequencing and agarose gel electrophoresis of the cell-line dilution model. An allele-specific PCR and surface hybridization based electrochemical detection method for SNP detection was proposed by Huang et al. (2012). Successful identification of single base mutations in human β -globin with a detection limit of 0.5 fM was reported.

Among these methods, the EIS analysis possesses the advantage of high sensitivity and short processing time. In this study, an EIS based nanostructured biosensor, with uniformly deposited GNPs as the sensing electrode, for effective detection of allergy gene mutation is proposed. In this device, an anodic aluminum oxide (AAO) barrier layer with a nanohemisphere array was used as the substrate. A gold thin-film was sputtered onto the AAO barrier-layer substrate to serve as the electrode for GNP deposition and sensing. A 70 mer gene fragment of the genome that is related to the expression of MD-2 was used for the detection of the gene mutation. The complementary target, containing 156 mer nucleotide, was prepared using the fresh blood from patients with allergic disease. An EIS analysis was implemented to discriminate between matching and mismatching of hybridizations for the capture probes and complementary targets.

2. Material and methods

2.1. Nanostructured impedance biosensor fabrication

The nanostructured impedance biosensor for the detection of SNPs is schematically illustrated in Fig. 1. The barrier-layer surface of an AAO membrane was adopted as the substrate. A gold thin-

film was sputtered onto the substrate, followed by a uniform electrochemical deposition of GNPs on the gold thin-film.

The fabrication details of the nanostructured biosensor are similar to those of previously reported work (Tsai et al., 2011) and are concisely depicted below. An AAO membrane was prepared using the conventional anodization process. A honeycomb-like surface barrier layer, containing convex honeycombs of around 80 nm diameter, was obtained after removing the remaining aluminum from under the barrier layer. The shape of the honeycombs on the surface of the barrier layer was further modified with 30-wt% phosphoric acid. An electrode consisting of a 10 nm Au thin film was sputtered onto the modified barrier-layer surface, using a radio frequency (RF) magnetron sputter. To make certain that the sensing area of each biosensor was consistent, a $\phi=6$ mm hole was punched into the center of a 2.5×2.5 cm² piece of parafilm, the bottom surface of the parafilm square was coated with a thin layer of AB glue, and the parafilm was adhered to the Au film barrier layer surface. Finally, a GNP layer was synthesized on the Au thin film by electrochemical deposition.

2.2. Probe and target DNAs preparation

A gene fragment that is related to the expression of MD-2 was used to probe the detection of a gene mutation in a patient. The sequence of the probe, as shown in Table 1, contains 70 mer of nucleotide. The 32nd nucleotide (C), indicated in bold, is the mutation location. The synthetic ssDNA of MD-2, with 0 base sequences shown in Table 1, was purchased from Tri-I Biotech, Taiwan. The target DNAs, as listed in Table 1, contain 156 mer of nucleotide and were prepared according to the genomic DNA mini kit protocol for fresh blood (Geneaid Biotech, Taiwan). The 79th nucleotide (T), indicated in bold, is the mutation location. It should be (G) for a normal person.

2.3. Immobilization of the ssDNA probe and hybridization of the complementary target

The process for ssDNA probe immobilization is detailed below. A 10 μ M probe-ssDNA solution was diluted 100-fold with phosphate-buffer saline (PBS), followed by uniform shaking. The diluted probe-ssDNA solution (30 μ L) was then dropped onto the electrode surface of the biosensor and incubated for 1 h. A 2 mM solution of 6-mercapto-1-hexanol (MCH) was added to the probe-ssDNA immobilized sample, in order to block the non-immobilized area. The sample was then incubated for 1 h and washed with PBS.

The hybridization process for the complementary target is described below. The genome specific DNA sample for allergic disease (complementary target) was magnified through a PCR process. Various numbers of PCR cycles (5, 10, and 20) were conducted to determine the minimum number of cycles required to produce sufficient amounts of the complementary target for

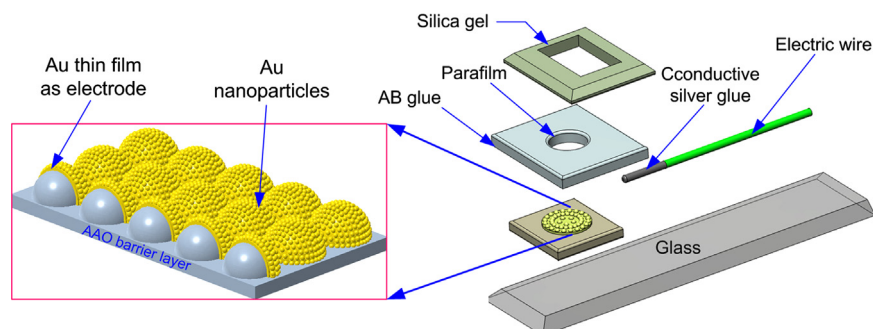


Fig. 1. Schematic illustration of the nanostructured biosensor.

Table 1
Base sequences of the probe and the target oligonucleotide sequences

| DNA sequence | Oligonucleotide sequence(5' to 3') |
|--------------------------------------|--|
| MD-2 9441 capture probe | GGTGAAGCGATTCTCCTGCCTCAGCCTCCCAGTAGCT GGGATTACAGGTGTGTGCCACCATGCCTGGC |
| MD-2 9441 complementary target | ACCTCACATCACCGGGTTAGAACCGAGTGACGTTGGA GACGGAGGACCCAACTTCGCTAAGAGGACGGAGTCGGA GGGTCATCGACCCCTAATGTCCACACACGGTGGTACGGA CCGATTAATAATAATAATCATCTCTGCCTTAAAGTT GTAC |

effective detection using the nanostructured biosensor shown in Fig. 1. The double-stranded reference (target) DNA solution was denatured at 95 °C for 10 min to form single-strand DNA. The solution of denatured target DNA was cooled to 50 °C, followed by uniform shaking. The diluted target DNA solution (30 μL) was then dropped onto the sensing device, which was incubated at 50 °C for 30 min and washed with PBS.

In the absence of a gene mutation in the reference DNA, all of the nucleotides in the selected DNA fragment matched with their corresponding nucleotides in the selected probe DNA fragment. However, if a gene mutation was present, then one of the nucleotides in the selected DNA fragment would not immobilize to the corresponding nucleotide in the selected probe DNA fragment.

2.4. Electrochemical analysis

An SP-150 potentiostat (Bio-Logic, USA) was implemented for the cyclic voltammetry (CV) analysis and electrochemical impedance spectroscopy (EIS) analysis. The EIS analysis was used to distinguish between DNA matching and mismatching through measurement of impedance differences. The working electrode, counter electrode and reference electrode were the nanostructured sensor, Pt film, and Ag/AgCl, respectively. A mixture of 5 mM Fe(CN)₆⁴⁻, 5 mM Fe(CN)₆³⁻ and 0.1 M KCl in 100 mM 2-(N-morpholino)-ethanesulfonic acid (MES) (pH=6.0) was used as the buffer solution. The applied DC power and AC power were 0 V and 10 mV, respectively. The scanning AC frequency was between 0.01 Hz and 100 kHz.

2.5. Elemental composition analysis

A PHI 5000 VersaProbe (ULVAC-PHI, Japan) X-ray photoelectron spectroscopy (XPS) instrument was used to analyze the elemental compositions of the electrode surface at each stage of immobilization.

3. Results and discussion

3.1. Sensor fabrication

Sensor fabrication results are displayed as SEM images of the AAO barrier layer and the GNP deposited hemispheric electrode array in Fig. S1. The diameter of the uniformly deposited GNPs shown in Fig. 2(b) was estimated to be 10–15 nm. Since the difference between a mutated and a non-mutated MD-2 allergy gene is very slight, it requires a highly sensitive biosensor to discriminate the difference. The high surface to volume ratio of the proposed nanostructured biosensor allows more probes to attach onto the electrode. Fig. S2 illustrates steady-state CVs for three different electrodes (AAO/Au/GNP, AAO/Au film, flat Au) in 20 mM Fe(CN)₆⁴⁻ and 0.1 M KCl at 100 mV/s versus Ag/AgCl reference

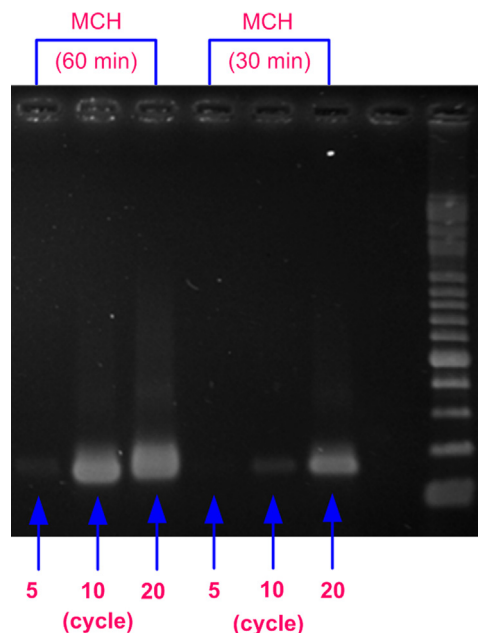


Fig. 2. Comparison of gel electrophoresis for the primers of complementary target and hybridized DNA.

electrode. The effective electrode area of the AAO/Au/GNP electrode is estimated to be 4.18-fold of the flat Au electrode.

3.2. Single-strand DNA probe immobilization and complementary target hybridization

3.2.1. ssDNA probe immobilization

The cyclic voltammograms for the GNP deposited and the ssDNA immobilized electrodes are displayed in Fig. S3. For the ssDNA probe immobilized electrode, both the peak anode current (I_{pa}) and the peak cathode current (I_{pc}) decreased, relative to the GNP deposited electrode. This result can be attributed to a drop in surface capacitance of the electrode due to the ssDNA probe immobilization. The CV results reveal that the ssDNA probes were effectively immobilized on the nanostructured electrode.

3.2.2. Complementary target hybridization

Various complementary target solutions, prepared by different PCR cycles, were used for hybridization experiments. When the hybridization was stable, sonication was conducted to detach hybridized DNA pairs. The primers for the complementary target were added to the solution containing sonicated DNA, followed by a 30 cycles PCR process to further magnify the complementary targets. Finally, gel electrophoresis was conducted to identify the complementary targets. Fig. 2 shows the results of the gel

electrophoresis for two MCH immobilization conditions. The gel electrophoresis results indicate that the hybridized DNA was the complementary target. The complementary target, which was produced by a 5 cycles PCR process, hybridized to the probe ssDNA after a 60 min MCH immobilization process.

3.2.3. Elemental composition analysis

Fig. 3 displays the XPS spectra for C, O, P and N with atomic orbital of C1s, O1s, P2p and N1s on the GNP deposited and ssDNA probe immobilized electrode surfaces, respectively. Based on the XPS spectra for P2p and N1s shown in Fig. 3(a) and (b), it was calculated that the area of the ssDNA probe immobilized electrode surfaces was 851.89 ($I \times eV$) and 1173.79 ($I \times eV$), respectively. In general, the XPS signals of N1s and P2p were not so strong when compared to that of the C1s and O1s (Lee et al., 2006). Furthermore, the used ssDNA was a 10 μM diluted 100-fold solution, the XPS signals of N1s and P2p were further attenuated. However, these results confirm the covalent immobilization of phosphorus and nickel.

3.3. Optimization of the probe ssDNA immobilization

To optimize the probe ssDNA immobilization, the original 10 μM probe ssDNA solution was diluted 10-, 100-, and 1000-folds. After immobilization of probe ssDNA, EIS was conducted to measure the variation in charge transfer resistance at different probe ssDNA concentrations.

The equivalent circuit shown in Fig. 4 was used to model the nanostructured biosensor that was used in this study, where R_{et} denotes the charge transfer resistance, R_s is the solution resistance, C is the double-layer capacitance, R_n represents the nanostructures resistance, Q models the constant phase element, and W is the Warburg impedance. R_{et} can be represented by the diameter of the Nyquist plot of the EIS analysis and can be used to indicate the resistance variations due to the DNA bindings.

To illuminate variations between different sensor substrates (AAO barrier layer), the R_{etp} ratio, defined as the charge transfer

resistance difference between the probe ssDNAs immobilized electrode and the bare nanostructured electrode ($\Delta R_{etp} = R_{etp} - R_{etb}$), divided by the charge transfer resistance of the original bare nanostructured electrode R_{etb} , was used. This ratio is an indicator for the evaluation of the optimal concentration for probe ssDNA on the nanostructured electrode. Fig. S4 shows various R_{etp} ratios, with respect to corresponding probe ssDNA concentrations. It was found that the values of the R_{etp} ratio for the 10- and 100-folds diluted probe ssDNA solutions are similar. The R_{et} saturated when a probe ssDNA concentration 100-fold diluted from the original 10 μM sample was used. This indicates that the 100-fold diluted probe ssDNA solution was sufficient to cover the surface of the nanostructured electrode.

3.4. Discrimination between matching and mismatching hybridizations

A total of 37 combined target samples from patients, including 19 gene mutated samples and 18 normal samples, were used for discrimination experiments. The mutation point for the gene mutated samples was verified by gel electrophoresis. Similar to the optimization of the probe ssDNA immobilization, the R_{ett} ratio, defined as the charge transfer resistance difference between the complementary target hybridized electrode and the probe ssDNAs immobilized electrode ($\Delta R_{ett} = R_{ett} - R_{etp}$), divided by the charge

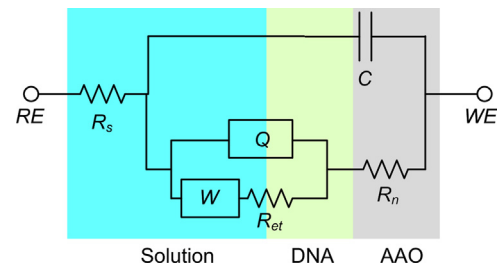


Fig. 4. Equivalent circuit for the nanostructured biosensor.

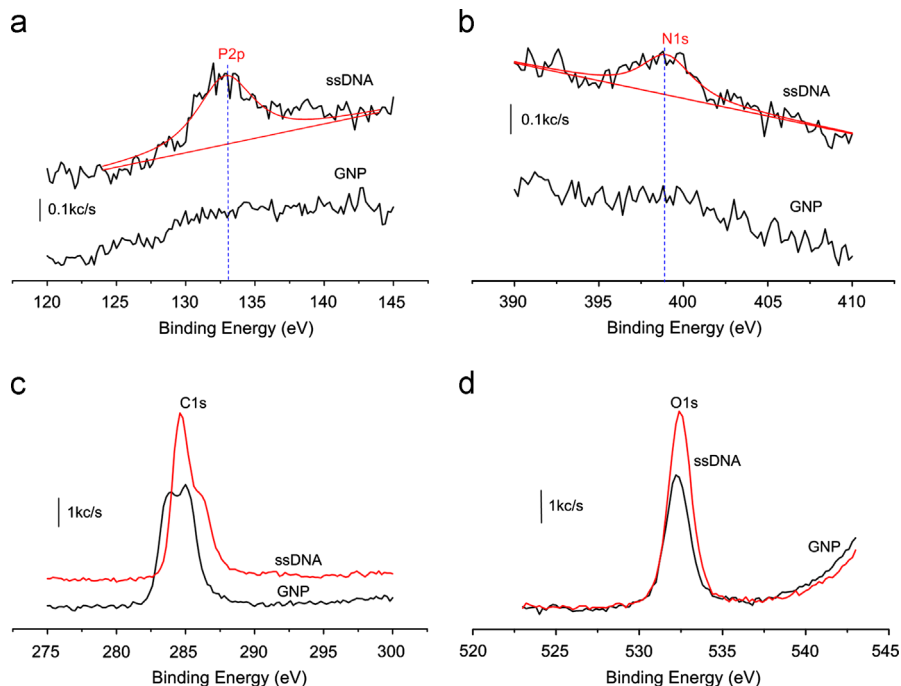


Fig. 3. XPS spectra for C, O, P and N on the GNP deposited and ssDNA probe immobilized electrode surfaces; (a), (b), (c) and (d) spectra for P2p, N1s, O1s, and C1s respectively.

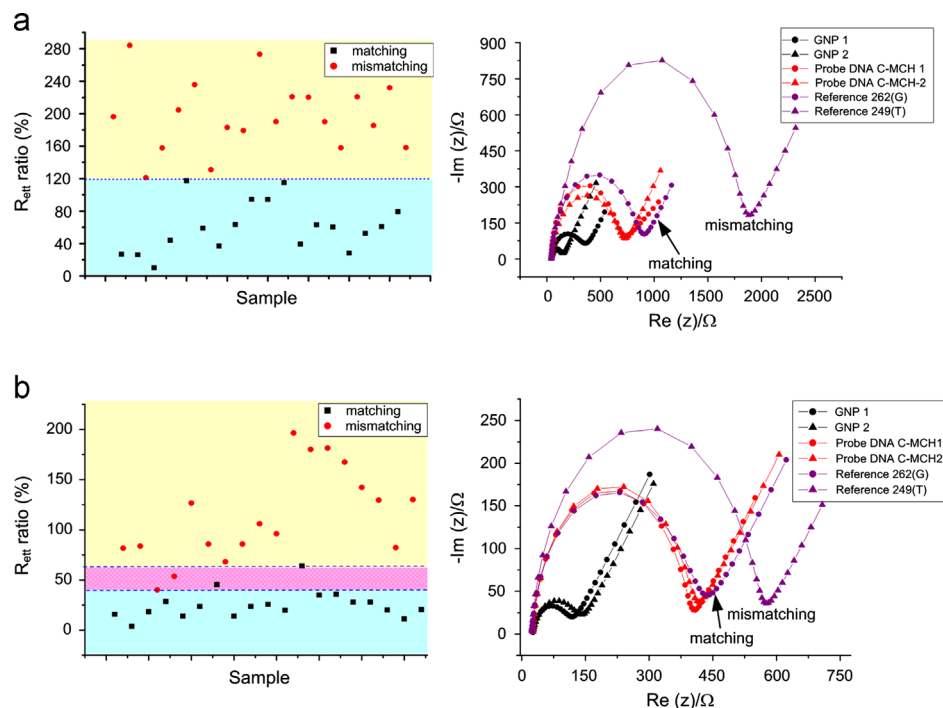


Fig. 5. Discrimination of matching and mismatching hybridizations of the 37 complementary targets that were produced by a 20 cycles PCR process; (a) complementary targets that were produced by a 20 cycles PCR process, R_{ett} ratio (matching) = $(59.7 \pm 30.8)\%$, and R_{ett} ratio (mismatching) = $(196.2 \pm 42.5)\%$ and (b) complementary targets that were produced by a 10 cycles PCR process, R_{ett} ratio (matching) = $(24.8 \pm 13.1)\%$, and R_{ett} ratio (mismatching) = $(113.3 \pm 46.0)\%$.

transfer resistance of the probe ssDNAs immobilized electrode R_{etp} , was used as the indicator for the discrimination between matching and mismatching hybridizations.

Fig. 5(a) displays the results of the discrimination experiments for the complementary targets that were produced by a 20 cycles PCR process. The measured impedance data are tabulated in Table S1(a). Based on Fig. 5(a), R_{ett} ratios of the matching hybridizations were less than 120%, while those of the mismatching hybridizations were larger than 120%. The results demonstrate that the nanostructured biosensor discriminated between mutated and non-mutated MD-2 allergy genes. The left figure displays the EIS analysis results for one of the matched and one of the mismatched samples.

Complementary targets produced by a shorter PCR process of 10 cycles and 5 cycles were used to investigate the limitations of the nanostructured biosensor. Fig. 5(b) shows the discrimination results for the complementary targets after a 10 cycles PCR process. The measured impedance data are tabulated in Table S1 (b). The results indicate that almost all of the SNPs for the complementary targets, after a 10 cycles PCR process, were detected by the nanostructured biosensor, except for one SNP from each group. The R_{ett} ratios of the matching hybridizations were less than 65%, while those of the mismatching hybridizations were larger than 40%. There were four overlaps out of 37 samples, including two matching samples and two mismatching samples. The relatively low R_{ett} ratios, when compared to those of the 20 cycles PCR processed complementary targets, can be attributed to a lower concentration of complementary target.

Full discrimination of complementary targets after a 5 cycles PCR process was not successful. It can be speculated that the concentration of the complementary targets after a 5 cycles PCR process was below the sensing limit of the nanostructured biosensor. In our future work, the microvibration method (Tsai et al., 2013) will be adopted to enhance the adhesion uniformity of the complementary targets so that PCR free discrimination can be achieved. More samples will be tested to verify the feasibility of

the nanostructured biosensor for the detection of base pairs in SNP of allergy genes.

4. Conclusion

In mammals, signaling of bacterial lipopolysaccharide (LPS), a major component of the cell wall of Gram-negative bacteria, proceeds through innate immune system (toll-like receptors: TLR). The MD-2 on the TLR acts as an essential component of the TLR/MD-2 receptor complex for microbial cell wall component recognition. The promoter, containing numerous transcription factor binding sites, is central to the regulation of gene transcription. There is growing evidence indicating that genetic variations in this region affect the transcription of target genes.

In this study, a sensitive nanostructured biosensor, based on uniformly deposited GNPs as the sensing electrode, for the effective detection of allergy gene mutation is presented. An AAO barrier-layer with a nanohemisphere array was used as the substrate, deposition of a gold thin film on the AAO barrier-layer substrate served as the electrode for GNP deposition. The MD-2 related 70 mer gene fragment was used to probe gene mutation. A total of 37 target samples from patients, including 19 mutated samples and 18 normal samples, were used for discrimination experiments. It was demonstrated that mutated and non-mutated allergy genes of MD-2 could be discriminated by the nanostructured biosensor; target samples were prepared with a 20 cycles PCR process.

Acknowledgment

The authors would like to offer their thanks to the Department of Health of Taiwan for their financial support of this research under Grant no. DOH101-TD-N-111-007.

Appendix A. Supporting information

Supplementary data associated with this article can be found in the online version at <http://dx.doi.org/10.1016/j.bios.2013.05.049>.

References

- Altshuler, D., Pollara, V.J., Cowles, C.R., Van Etten, W.J., Baldwin, J., Linton, L., Lander, E.S., 2000. *Nature* 407, 513–516.
- Cooper, D.N., Smith, B.A., Cooke, H.J., Niemann, S., Schmidtke, J., 1985. *Human Genetics* 69, 201–205.
- Drabovich, A.P., Krylov, S.N., 2006. *Analytical Chemistry* 78, 2035–2038.
- Ensafi, A.A., Taei, M., Rahmani, H.R., Khayamian, T., 2011. *Electrochimica Acta* 56, 8176–8183.
- Griffin, T.J., Smith, L.M., 2000. *Analytical Chemistry* 72, 3298–3302.
- Huang, Y., Zhu, J., Li, G., Chen, Z., Jiang, J.H., Shen, G.L., Yu, R.Q., 2012. *Biosensors and Bioelectronics* 42C, 526–531.
- Ingebrandt, S., Han, Y., Nakamura, F., Poghossian, A., Schoning, M.J., Offenhausser, A., 2007. *Biosensors and Bioelectronics* 22, 2834–2840.
- Kerman, K., Saito, M., Morita, Y., Takamura, Y., Ozsoz, M., Tamiya, E., 2004. *Analytical Chemistry* 76, 1877–1884.
- Lee, C.H., Gong, P., Harbers, G.M., Grainger, D.W., Castner, D.G., Gamble, L.J., 2006. *Analytical Chemistry* 78, 3316–3325.
- Luo, X., Hsing, I.M., 2009. *Biosensors and Bioelectronics* 25, 803–808.
- Miyake, K., 2004. *Trends in Microbiology* 12, 186–192.
- Palchetti, I., Berti, F., Laschi, S., Marrazza, G., Mascini, M., 2010. *Sensors and Microsystems*. In: Malcovati, P., Baschiroto, A., d'Amico, A., Natale, C. (Eds.), Springer, Netherlands, pp. 181–184.
- Situ, B., Cao, N., Li, B., Liu, Q., Lin, L., Dai, Z., Zou, X., Cai, Z., Wang, Q., Yan, X., Zheng, L., 2012. *Biosensors and Bioelectronics* 43C, 257–263.
- Tsai, J.J., Bau, I.J., Chen, H.T., Lin, Y.T., Wang, G.J., 2011. *International Journal of Nanomedicine* 6, 1201–1208.
- Tsai, J.J., Liu, Y.F., Liao, E.-C., Chen, J.L., Wang, G.J., 2013. *Sensors and Actuators B: Chemical* 178, 404–411.
- Zhang, S., Wu, Z., Shen, G., Yu, R., 2009. *Biosensors and Bioelectronics* 24, 3201–3207.